Biochemical Pharmacology 80 (2010) 136–143

Contents lists available at ScienceDirect

Biochemical Pharmacology

journal homepage: www.elsevier.com/locate/biochempharm

Biochemical characterization of the binding of cyclic RGDyK to hepatic stellate cells

Xiao-wei Huang [a], Ji-Yao Wang [a,*], Feng Li [a], Zheng-Ji Song [a], Cao Xie [b], Wei-Yue Lu [b]

[a] Department of Gastroenterology, Zhongshan Hospital affiliated to Fudan University, 180 Feng Lin Road, Shanghai 200032, China
[b] Fudan-PharmCo Targeting Drug Research Center, School of Pharmacy, Fudan University, Shanghai 200032, China

ARTICLE INFO

Article history:
Received 26 January 2010
Accepted 11 March 2010

Keywords:
Liver fibrosis
Hepatic stellate cell
Integrin αvβ3
cRGDyK peptide
Targeted binding

ABSTRACT

Activated hepatic stellate cells (HSCs) play a crucial role in the development of liver fibrosis. Noninvasive monitoring of the activation of HSCs has been challenging due to the lack of specific receptors or motifs on the cells. The present study provides the evidence that integrin αvβ3 expressed on HSCs is a biomarker reflecting the activation of HSCs. Solid-phase synthesis of cRGDyK (Arg-Gly-Asp-$_D$Tyr-Lys) peptide and FAM-conjugated peptide were employed for binding to integrin αvβ3. The increased expression of integrin αv and β3 at mRNA and protein levels was detected during HSC activation. The affinity of cRGDyK to integrin αvβ3 was examined by both radioligand binding assay and FAM-conjugated peptide binding measurements. Quantitative RT-PCR and Western blotting showed a less dramatic, but significant increase in αv and β3 integrin mRNA and protein expression following activation of rat HSCs. Radioiodinated cRGDyK binds to both purified and membrane-bound integrin αvβ3 with high affinity in a dissociable manner. FAM-conjugated cRGDyK was coupled to activated HSCs in a time- and dose-dependent, receptor-mediated manner. Activated HSCs express sufficient number of integrin αvβ3 receptor. cRGDyK peptide binds to both purified and membrane-bound integrin αvβ3 with high affinity in a reversible fashion. Thus, the cRGDyK peptide represented a new agent potentially useful for the diagnosis of liver fibrosis.

1. Introduction

Perisinusoidal hepatic stellate cells (HSCs) play an essential role in the development of liver fibrosis. Targeting HSCs for drug delivery or a diagnostic purpose has been much more difficult than hepatocytes and Kupffer cells due to no specific motifs or receptors existing on the cell surface, relatively fewer cell numbers, and residence of HSCs in the Disse space side of SECs [1,2]. In recent years, research concerning phenotype conversion of HSCs offers the possibility to develop targeting diagnostic and therapeutics for hepatic fibrosis [3–5]. In the normal liver, quiescent HSCs have a low proliferative rate and maintain a phenotype with less extraceullar matrix production. However, following chronic liver injury HSCs undergo profound alterations in morphology and synthetic capabilities, transforming to proliferative myofibroblastic cells expressing a wide range of collagenous and noncollagenous extracellular matrix (ECM) molecules as well as the characteristic marker smooth muscle α-actin (SMA) [6–8].

Integrins are a family of heterodimeric cell surface receptors that regulate cell attachment and respond to the extra-cellular matrix [9]. Among all 24 integrins discovered to date, the integrin αvβ3 is the most extensively studied. The integrin αvβ3 plays an important role in angiogenesis and tumor metastasis, and is expressed on activated endothelial cells as well as on some tumor cells [10]. Therefore, a number of different approaches using αvβ3 as an imaging modality have been explored for targeting tumors, including positron emission tomography (PET), single photon emission tomography (SPECT), magnetic resonance imaging (MRI), optical imaging and ultrasound using targeted microbubbles [11–20]. However, no study available employing integrin αvβ3 as a marker for targeting activated HSCs for diagnostic or therapeutic attempts.

The role of αvβ3 integrin in activation of HSC, the effector cells of liver fibrosis, remained largely unexplored. HSCs were shown to express integrins α1β1, α2β1, αvβ1, α6β4 [21], αvβ3 [22], α5β1 [23,24], α8β1 [25]. Previous study showed that αvβ3 integrin was

Abbreviations: HSC, hepatic stellate cell; DMEM, Dulbecco's minimal Eagle's medium; FBS, fetal bovine serum; GAPDH, glyceraldehyde-3-phosphate dehydrogenase; Ct, cycle threshold; PBS, phosphate-buffered saline; ECM, extracellular matrix; cRGDyK, cyclo-(Arg-Gly-Asp-DTyr-Lys); FAM, carboxyfluorescein; cRGAyK, cyclo-(Arg-Gly-Ala-DTyr-Lys); DAPI, 4,6-diamidino-2-phenylindole; RT-PCR, reverse transcriptase-polymerase chain reaction.

* Corresponding author. Tel.: +86 21 64041990x2117; fax: +86 21 64432583.
E-mail addresses: wang.jiyao@gmail.com, wang.jiyao@zs-hospital.sh.cn (J.-Y. Wang).

0006-2952/$ – see front matter © 2010 Elsevier Inc. All rights reserved.
doi:10.1016/j.bcp.2010.03.015

expressed by activated myofibroblastic rat and human stellate cells in culture, and it modulates HSC survival and proliferation [22].

Since several ECM proteins like vitronectin, fibrinogen and fibronectin interact with integrins via the RGD sequence, linear as well as cyclic RGD-peptides have been designed to function as αvβ3-specific ligands. Kessler and co-workers developed the pentapeptide cRGDyK (–Arg-Gly-Asp-DTyr-Lys–), which shows a high affinity and selectivity for αvβ3 coupling, is the most prominent structure for the development of molecular imaging compounds for the determination of αvβ3 expression [26].

The aim of the present study was to characterize the binding specificity and capability of cRGDyK to purified integrin αvβ3 and membrane-bound integrin αvβ3 on activated HSCs. Our findings provided the evidence that integrin αvβ3 is an biomarker reflecting activation of HSCs. Cyclic RGDyK peptide may facilitate the development of molecular imaging agents for the diagnosis and monitoring the progression of liver fibrosis.

2. Materials and methods

2.1. Animals

Male SD rats (250–300 g) were obtained from Shanghai Institute of Material Medicine, Chinese Academy of Science. The protocol of animal experiments was approved by the Institutional Ethical Committee of Animal Experimentation, and the experiments were performed strictly according to the governmental and international guidelines on animal experimentation.

2.2. Chemicals

All the amino acids used in peptide synthesis were purchased from PE Biosystems in prepacked tubes except for the Fmoc-D-Tyr-OH and Fmoc-Lys(Mtt)-OH, which were supplied by Novabiochem (San Diego, CA). The other peptide synthesis reagents were also obtained from PE Biosystems. The TFA was purchased from Pierce Chemical while the other cleavage reagents were obtained from Aldrich. Fluoresceine isothiocyanate (FITC) were purchased from Sigma Chemical Co. (St. Louis, MO). DMEM, fetal bovine serum, L-glutamine, penicillin and streptomycin were purchased from Gibco-BRL (Gaithersburg, MD). Nonidet P-40, echistatin, pronase and collagenase were purchased from Sigma Chemical Company (St. Louis, MO). Human integrin αvβ3 purified protein was purchased from Millipore (Boston, MA). All reagents were of analytical grade and were used without further purification.

2.3. Synthesis of cyclic pentapeptide c(RGDyK) and fluorescence labeling

Cyclic RGD peptide c(RGDyK) (M_w = 619.6) was synthesized via a Fmoc-protected solid phase peptide synthesis strategy. 9-Fluorenylmethoxycarbonyl (Fmoc) amino acids and 2-chlorotrityl chloride resin were purchased from Novabiochem (San Diego, CA). Arginine and lysine were protected from hydrolysis by the 2,2,4,6,7-pentamethyldihydro-benzofuran-5-sulfonyl (Pbf) and tert-butoxycarbonyl (Boc) groups, respectively, while D-tyrosine and aspartic acid were protected as a tert-butyl ester. Glycine was chosen as the C-terminal amino acid in order to avoid a racemization in the cyclization step. The coupling agents were 2-(1H-benzotriazol-1-yl)-1,1,3,3-tetramethyluronium tetra-fluoroborate (HBTU)/1-hydroxytriazole (HOBt)/N,N-diisopropylethylamine (DIEA). The resulting fully protected linear pentapeptide H-Asp(OtBu)-D-Tyr(OtBu)-Lys(Boc)-Arg(Pbf)-Gly-OH, was cyclized by PyBOP and deprotected by trifluoroacetic acid (TFA). Purification was applied on Waters Delta 600 Prep system equipped with Waters Symmetry C18 column (19 mm × 300 mm). The eluent solvents were water containing 0.1% TFA (solvent A) and acetonitrile containing 0.1% TFA (solvent B).

Labeling cRGDyK (M_w = 1009.4) with fluorescence was carried out by mixing the cRGDyK with FITC for 3 h in DMF at room temperature and purified in the same manner as described before. The lyophilized product was redissolved in sterile ultra pure water at a concentration of 1 mg/ml and stored in the dark at −80 °C.

2.4. Radioiodination of cRGDyK used for binding assays

cRGDyK was labeled with [^{125}I]iodide at a position ortho to its D-Tyr (y) phenol group using the chloramine-T method previously described with some modification. Briefly, cRGDyK (100 μg, 0.13 μmol/50 μl water) was reacted with [^{125}I] NaI (37.0 MBq) and 0.5 M phosphate buffer solution (pH 7.4, 100 μl). To this solution, chloramine T (30 μg, 1.3 μmol/0.1% solution in 0.05 M phosphate buffer solution, pH 7.4) was added. Two min after adding chloramine, the reaction was quenched with $Na_2S_2O_5$ (60 μg, 0.32 μmol/0.1% solution in 0.05 M phosphate buffer solution, pH 7.4). The crude mixture was purified by semi-preparative HPLC (from 5% EtOH/0.05% TFA solution to 30% EtOH/0.05% TFA solution gradient over 20 min at 3 ml/min) to afford [^{125}I]iodo-c(RGDyK) (tRet = 15.3 min) [27].

2.5. Isolation of rat hepatic stellate cells

Rat HSCs were extracted from normal rat liver using pronase and collagenase as described previously [28]. HSCs were purified to 90–95% purity by density gradient centrifugation and elutriation. Purified HSCs were cultured on plastic culture dishes for 10–14 days to induce activation to a smooth muscle α-actin-positive myofibroblastic phenotype. Unless otherwise stated, rat HSCs were used for our studies after activation in primary culture for ~14 days or after the first or second passage. Cells were cultured in Dulbecco's modified Eagle's medium in the presence of 10% fetal bovine serum and penicillin and streptomycin.

2.6. Immunofluorescent staining of smooth muscle α-actin (SMA) in HSCs

For fluorescent staining, the activated HSCs cultured on cover-slips were washed with PBS, fixed in 3% paraformaldehyde in PBS for 30 min, and then incubated in 0.1% Triton X-100 in PBS for 15 min. Immunohistochemistry was performed for the detection of SMA using indirect immunofluorescence with a primary mouse monoclonal anti-SMA antibody from Sigma (St. Louis, MO, USA) at a dilution of 1:100 in PBS/1.0% BSA and an FITC-conjugated secondary goat anti-mouse antibody from Invitrogen Corporation (Carlsbad, CA, USA), at a dilution of 1:200 in PBS/1.0% BSA. Following secondary antibody staining, samples were rinsed in PBS/1.0% BSA for 10 min then incubated with 4′,6-diamidino-2-phenylindole, dihydrochloride (DAPI) at a dilution of 1:1000 in PBS/1.0% BSA for 5 min at room temperature (RT) to reveal cell nuclei. After two 10-min rinses in PBS/1.0% BSA, samples were overlaid with a #1.5 glass cover-slip (Fisher Scientific, Pittsburgh, PA, USA) using 50% glycerol in PBS with 1% N-propylgallate as a mounting medium. After mounting, the slides were viewed using a fluorescence microscope (Carl Zeiss, Oberkochen, Germany).

2.7. RNA extraction and qRT-PCR analysis

Total RNA was extracted from the cultured cells, quantified by absorbance at 260 nm, normalized, and reverse-transcribed into first-strand complementary DNA (cDNA). Amplification and detection were performed using the ABI PRISM 7900 Sequence

Detection System (Applied Biosystems, Foster City, CA) starting with 1 μl cDNA and SYBR Green qRT-PCR Master Mix (Toyobo, Japan) [29]. Rat glyceraldehyde 3-phosphate dehydrogenase (GAPDH) was used as an internal standard. Primers of GAPDH: sense, 5′-GGCATCCTGGGCTACACTGA-3′; antisense, 5′-GCCAGCCCCAGCATCA-3′; these primers were as follows: integrin β3: sense, 5′-CTATGGAGACACCTGCGAGAAGT-3′; antisense, 5′-CTTACACTCCACACAGTCCTTCTTAAA-3′; integrin αv: sense, 5′-GCTGAGCAAGGAGGAAGAAATC-3′; antisense, 5′-CACAGCCCAAAGTGTGAACATC-3′; the relative expression of integrin β3 and integrin αv messenger RNA (mRNA) was analyzed by the comparative cycle threshold (Ct) method. Melting curve analysis and visualization of PCR-products on agarose gel were performed to ensure specificity of qRT-PCR. All experiments were performed in triplicate.

2.8. Western blotting

Protein was extracted from the cultured hepatic stellate cells. Protein samples (50 μg) were separated by 8, 10 or 12% SDS-PAGE, transferred to polyvinylidene difluoride membranes (Gelman-Pall, Ann Arbor, MI, USA), blocked with 5% nonfat milk, and incubated with either rabbit polyclonal antibodies against integrin αv (1:1000; Abcam, MA), or rabbit polyclonal antibodies against integrin β3 (1:1000; Abcam, MA) or mouse monoclonal antibodies against GAPDH (1:1000; Sigma, St. Louis, MO) respectively, at 4 °C. After washing, the membrane was incubated with horseradish peroxidase-conjugated anti-mouse IgG (1:1000) or anti-rabbit IgG (1:1000) (all from Calbiochem, CA) for 1 h at room temperature. Chemiluminescent signals were generated by the addition of the SuperSignal West Pico Chemiluminescent Substrate (Pierce, Rockford, IL) and detected on a radiographic film. Where shown, scanning densitometry analysis was used to quantitate relative expression with Phoretix Advanced 1D software (Non-Linear Dynamics Ltd., Newcastle, UK).

2.9. Solid-phase receptor binding assay

The receptor binding assay was performed as described previously [30], with slight modification. Human integrin αvβ3 purified protein was diluted at 500 ng/ml in coating buffer (20 mM Tris, pH 7.4, 150 mM NaCl, 2 mM $CaCl_2$, 1 mM $MgCl_2$, 1 mM $MnCl_2$) and an aliquot of 100 μl/well was added to a 96-well micro-titer plate (Microlite-2 from Dynatech) and incubated overnight at 4 °C. The plate was washed once with blocking/binding buffer (50 mM Tris, pH 7.4, 100 mM NaCl, 2 mM $CaCl_2$, 1 mM $MgCl_2$, 1 mM $MnCl_2$, 1% bovine serum albumin), and incubated an additional 2 h at room temperature. The plate was rinsed twice with the same buffer and incubated with radiolabeled ligand at the indicated concentrations for 3 h at room temperature. For coincubations, unlabeled competitor was included at the concentrations described. For preincubations, after the 3 h incubation with radiolabeled ligand, the plate was washed three times with blocking/binding buffer and further incubated for indicated times in the presence of either competitor or buffer alone. After an additional three washes, the plates were counted by liquid scintillation method with Top count (Packard, Meriden, CT). When ^{125}I-cRGDyK incubations were performed without receptor, weak interaction was detected because of nonspecific adsorption with the micro-titer well. Nonspecific binding of ligand to the receptor was determined with molar excess (500-fold) of the unlabeled ligand. Each data point is a result of the average of triplicate wells.

2.10. Radioligand binding measurements

To determine the affinity of ^{125}I-cRGDyK for αvβ3 integrin on hepatic stellate cells, binding isotherms of integrin αvβ3 expressed on activated HSCs and radiolabeled cRGDyK were generated. Radiolabeled cyclic RGDyK at 2000 Ci/mmol (Amersham, Chicago, IL) was used. For binding assays, cells were harvested and resuspended (2×10^6 cells/ml) in adhesion buffer containing 1 × Hanks' balanced salt solution lacking divalent cations, 50 mM HEPES (pH 7.4), 1 mg/ml of bovine serum albumin, 0.5 mM $MnCl_2$ and 2 mM $CaCl_2$. A concentration range of ^{125}I-cRGDyK was added to the HEK-293 (αvβ3 negative) or the HSC (αvβ3 positive) cells in suspension (2×10^5 cells/well) in 96-well microtiter plate (Falcon Microtest III) and the mixture was incubated for 2 h by shaking at room temperature. At the end of the incubation period, the cells were filtered with use of Millipore Multiscreen-FB (glass fiber type B) plates which had been pretreated with 100 ml of 0.3% polyethylenimine solution for 2 h. The filters were then washed three times with 100 ml of adhesion buffer. The plates were allowed to dry and the individual filters were punched out and counted in a gamma counter. Nonspecific binding was measured in the presence of 500-fold molar excess of cRGDyK. Each data point is an average of values from triplicate wells. All measurements were repeated at least three times. Bound ligand was calculated from the nonspecific and total radioactivity of the ligand and the results are presented as picomoles bound per million cells. The binding affinity (K_d) of cRGDyK was calculated by analyzing the data with nonlinear regression by use of GraphPad Prism (version 5). The K_d and B_{max} values were also displayed by Scatchard plot.

2.11. Binding of cyclic RGD peptides to HSCs

FAM-conjugated cRGDyK or cRGAyK peptides were incubated at concentrations of 0.04–125 μM with quiescent or activated HSCs (1×10^6 cells/well) at either 4 °C for 1 h or 37 °C for 15–90 min. After the incubation, the cells were washed three times with ice-cold binding buffer, pH 7.4. The FAM-positive cells were counted by flow cytometry, and the data are expressed as percentage of counted cells.

In separate experiments, cells were plated at 2×10^6 cells/well in 6-well plates, and they were incubated with FAM-conjugated cRGDyK or cRGAyK peptides at 2 μM for 1 h. After washing three times with binding buffer and staining by 4,6-diamidino-2-phenylindole (DAPI), the cells were visualized under a confocal microscope (Leica TCS SP2 AOBS, USA). Cells were optically sectioned, and digital images were acquired. All instrumental parameters pertaining to fluorescence detection, and image analyses were held constant to allow sample comparison.

2.12. Statistical analysis

Quantitative data are presented as the mean ± SD. The mRNA and protein levels were normalized to the mean of control data in each set of experiments. Comparison between the groups was performed by one-way analysis of variance (ANOVA), followed by Tukey's test. In all cases, a p value of <0.05 was taken to indicate statistical significance.

3. Results

3.1. Peptide synthesis and radiolabeling

The cyclic RGD peptide was prepared by solid-phase synthesis of linear peptide sequences, using the Fmoc protection strategy, followed by cyclization and side-chain deprotection in solution. To minimize steric hindrance and racemization, the linear, side-chain-protected peptide was assembled with the glycine at the C-terminus. The Fmoc-protected amino acids were coupled with HBTU/HOBt in the presence of DIEA as base. The super-acid labile

o-chlorotrityl resin was chosen as the solid support. The fully protected linear peptide H-Gly-Asp(OtBu)-$_D$-Tyr(OtBu)-Lys(Boc)-Arg(Pbf)-OH was produced under mildly acidic conditions (HOAc/TFE/DCM = 1:1:8 or 1% TFA in DCM). The filtrate was immediately neutralized with pyridine to avoid side-chain deprotection. Crude, unpurified product was cyclized in DMF solution (0.05 M) with HBTU/HOBt in the presence of DPPA/$NaHCO_3$ (or 2,4,6-collidine) as base at room temperature for 24 h. After solvent removal, the fully protected cyclic peptide was isolated by flash chromatography, with 55% yield. Side chain deprotection was achieved in almost quantitative yield by treating the product with TFA in the presence of free radical scavenger (triisopropylsilane). Purification by reversed-phase high-performance liquid chromatography (RP-HPLC) yielded the desired peptide, which was >98% in purity (as determined by analytical HPLC with monitoring at λ = 218 nm). The product was further characterized by ESI mass spectroscopy.

Head-to-tail cyclization on resin was also successful. This strategy starts with loading of Fmoc-Asp-OAll onto NovaSyn® PEG resin (0.22 mmol/g loading efficiency). Following standard amino acid assembly and Fmoc deprotection with DBU/piperidine, the on-board cyclization was achieved using $Pd(PPh_3)_4$ mediated removal of allyl protection followed by carboxyl activation. Finally, cleavage and deprotection were accomplished with Reagent K (85% TFA/5% thioanisole/5% phenol/5% water). Due to the extremely low yield of on-resin cyclization and the expense of the α-allyl ester of Fmoc-Asp, we adopted the solution cyclization method over the solid-phase cyclization method.

Radiochemical yields of ^{125}I-RGD ranged from 70 to 90% and radiochemical purity was ≥95%. ^{125}I-RGD was prepared with high specificity of activity, since the retention time of ^{125}I-RGD (13.5 min) was well separated from that of the RGD. HPLC purification with 0.5 ml/fraction collection enabled the isolation of ^{125}I-RGD with specific activity of 2000 Ci/mmol provided fresh [^{125}I]NaI was used for the radiolabeling.

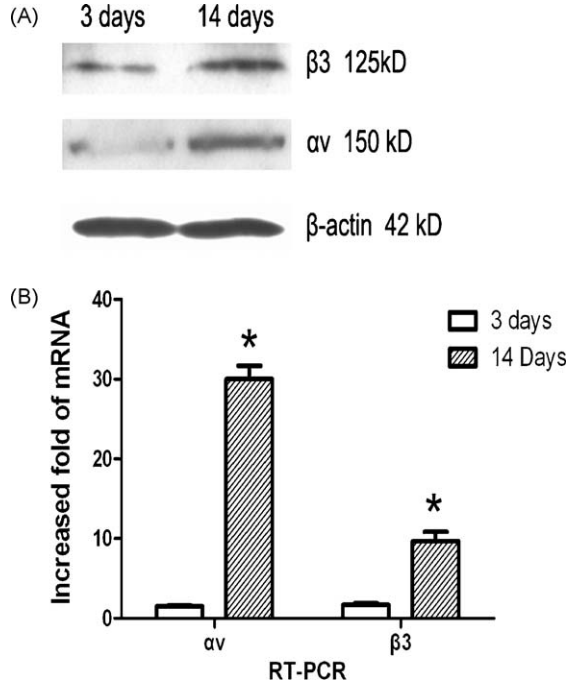

Fig. 1. Expression of integrin αvβ3 by rat HSCs. (A) Quiescent rat hepatic stellate cells (3d) or HSCs activated by culture for 14 days on plastic (14d) of which proteins were extracted and subjected to Western blotting for β3 or αv expression. (B) Expression of mRNA for integrin αv and β3 in quiescent (3d) rat HSCs or rat HSCs activated on plastic for 14 days (14d) was detected by qRT-PCR and normalized to GAPDH mRNA expression. Data are the mean of three independent experiments. $^*p < 0.05$.

3.2. HSCs express αvβ3 integrin following activation in vitro

Freshly isolated HSCs (quiescent HSCs) from rat liver were induced to activate to a myofibroblastic phenotype by culture on plastic culture wells for 14 days. Detection of αv and β3 integrin in cell lysates by Western blotting showed that its expression was increased 6.7- and 4.3-fold, respectively, after 14 days of culture activation on plastic vessels (Fig. 1A). Whereas mRNA expression of αv and β3 integrin was increased up to 20- and 5.7-fold following activation of rat HSCs at the same time points (Fig. 1B).

3.3. Binding of cRGDyK to purified αvβ3 receptor

To characterize the binding of cRGDyK to integrin αvβ3 receptors in detail, we used the purified human integrin αvβ3 protein. The binding of cRGDyK to purified αvβ3 was measured by a solid-phase receptor binding assay. As shown in Fig. 2A, ^{125}I-cRGDyK bound to purified αvβ3 in a saturable and specific manner, because it was effectively inhibited by coincubation with cold cRGDyK. Incubation of αvβ3 receptor (50 ng) with increasing concentrations of ^{125}I-cRGDyK resulted in a saturable binding. Nonspecific binding was evaluated by carrying out the binding assay in the presence of a 500-fold molar excess of cRGDyK and was typically less than 10% of the total binding (Fig. 2A). Nonlinear regression analysis of the binding data gave a fit with a K_d of 0.97 nM and B_{max} of 1049 pmol/mg protein as determined by GraphPad Prism (version 5). The data were also displayed by Scatchard plot (Fig. 2B).

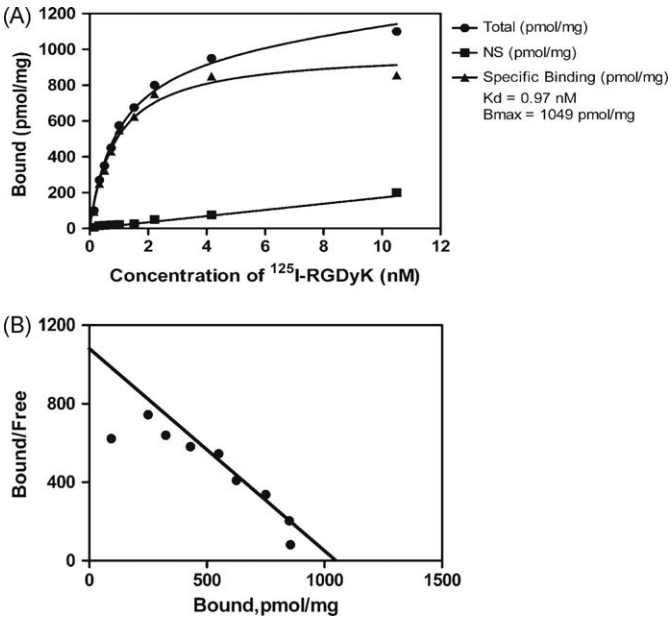

Fig. 2. Saturation binding isotherm for binding of ^{125}I-cRGDyK to αvβ3. (A) Saturation binding isotherms of ^{125}I-cRGDyK to αvβ3 receptor were determined in a solid-phase receptor binding assay as described under Section 2.7. Human integrin αvβ3 purified protein was coated at a concentration of 10 ng/well onto Microlite-2 plates and incubated with various concentrations (0.05–5 nM) of ^{125}I-cRGDyK for 3 h at room temperature. Bound ligand concentration was determined by solubilizing the counts with boiling 2N NaOH and was subjected to gamma counting. Nonspecific binding was evaluated by carrying out the binding assay in the presence of 500-fold molar excess of cold cRGDyK (●, total binding; ▲, specific binding; ■, nonspecific binding). Each data point is an average of triplicate measurements in which the error was less than 5% of the total binding. To derive the affinity of the interaction between cRGDyK and αvβ3, the data shown in panel (A) were analyzed by nonlinear regression analysis with the GraphPad Prism program (Version 5). (B) The data shown in panel (A) were also displayed according to the method of Scatchard plot.

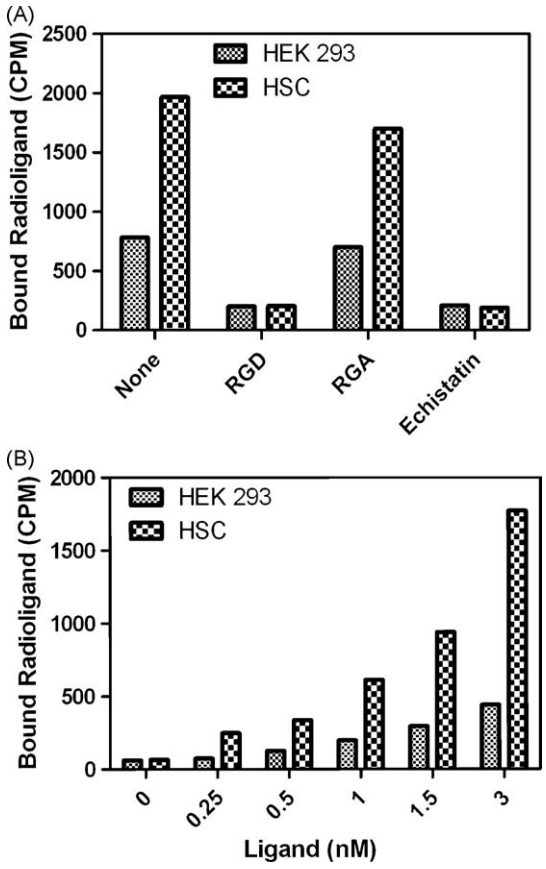

Fig. 3. Binding of ^{125}I-cRGDyK to$\alpha v\beta 3$ expressed on HSCs. (A) HSCs ($\alpha v\beta 3$ integrin positive) and HEK-293 cells ($\alpha v\beta 3$ integrin negative) were harvested from tissue culture flasks and were re-suspended in adhesion buffer containing 1 mM Mn^{++}. ^{125}I-cRGDyK (1 nM) was added to the cells in the presence of competitors. Cold cRGDyK peptide (5 nM), cRGAyK peptide (500 nM) and echistatin (500 nM) were added to the cells before the addition of radioligand and the mixture was allowed to incubate with shaking for 2 h at room temperature. Bound ligand was separated from free ligand by filtration through microtiter plates with glass fiber filters at the bottom of the wells, as described under Section 2.8. The wells were washed and radioactivity was determined by punching the membranes out and counting by gamma counting. Each point is the average of triplicate data points and the results shown are a representative of at least three experiments. (B) HSCs and HEK-293 cells (2×10^5 cells/well) were incubated with increasing concentration of ^{125}I-cRGDyK for 2 h at room temperature and the bound ligand was estimated as described above.

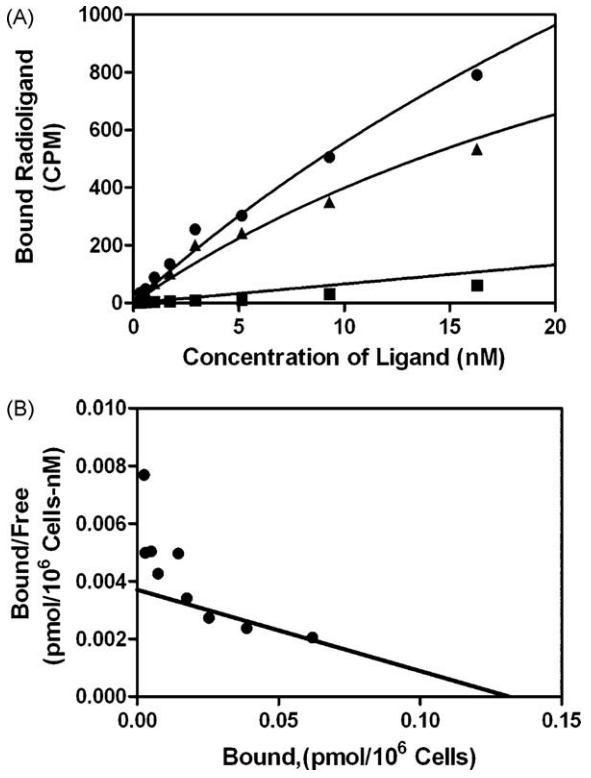

Fig. 4. A measurement of the binding affinity between ^{125}I-cRGDyK and $\alpha v\beta 3$ expressed on HSCs. (A) Isotherms of ^{125}I-cRGDyK binding to activated HSCs maintained in suspension were generated. Cells were harvested from tissue culture flasks and were re-suspended in adhesion buffer containing 1 mM Mn^{++}. ^{125}I-cRGDyK of increasing concentration was added to the cells and the mixture was allowed to incubate with shaking for 2 h at room temperature. Bound ligand was separated from free ligand by filtration as described above. Each point is the average of triplicate data points, and the isotherm shown represents at least three experiments (●, total ^{125}I-cRGDyK bound to the receptor; ▲, specific binding; ■, nonspecific binding). To derive the number of receptors expressed on HSCs, the data shown in panel (A) were analyzed by nonlinear regression analysis with the GraphPad Prism program (Version 5). (B) The data were also replotted according to the method of Scatchard. B_{max} is the *x*-intercept.

3.4. Binding of cRGDyK to $\alpha v\beta 3$ expressed on HSCs

To measure the binding of cRGDyK to $\alpha v\beta 3$ expressed on the cell surface, hepatic stellate cells (HSCs) were harvested from culture flasks, placed in suspension and incubated with ^{125}I-cRGDyK for 2 h. Human embryonic kidney 293T cells (HEK-293) that are negative for $\alpha v\beta 3$ expression were used as a negative control in these experiments. The binding rate of HSCs to radiolabeled cRGDyK was 2.36-fold higher than $\alpha v\beta 3$ negative HEK-293 cells. The binding of ^{125}I-cRGDyK to HSCs was inhibited by cold cRGDyK peptide and echistatin, but not by the peptide containing the RGAyK sequence (Fig. 3A). Addition of increasing concentrations of radioligand to the cells resulted in a linear increase in the total amount of radioligand bound to the HSCs (Fig. 3B). To measure the affinity of ^{125}I-cRGDyK to $\alpha v\beta 3$ receptor expressed on HSCs, binding isotherms were generated in a concentration range of ^{125}I-cRGDyK (Fig. 4A) as described under Section 2.10. Nonspecific binding was evaluated by carrying out the binding assay in the presence of 500-fold molar excess of cold cRGDyk and was typically less than 5% of the total binding. Nonlinear regression analysis of the binding isotherms revealed that the number of cell surface binding sites is 79,042 sites per cell (Fig. 4A). The data was also displayed by Scatchard plot (Fig. 4B).

3.5. Selective binding of FAM-conjugated cRGDyK to HSCs

To determine the affinity of the cRGDyK with HSCs, quiescent and activated HSCs were incubated with FAM-conjugated cRGDyK or cRGAyK peptides. The FAM-positive HSC number was significantly increased when the FAM-conjugated cRGDyK concentration was elevated from 0.04 μM to 125 μM (Fig. 5A), suggesting that the binding of cRGDyK with activated HSCs was boosted with the elevation in peptide concentration. Meanwhile, the combination of the peptide with HSCs seemed to be time-dependent, because the relative fluorescent intensity was increased when incubation time was extended from 15 min to 90 min (Fig. 5B).

The affinity of cRGDyK to HSCs was further evaluated under a confocal microscope (Leica TCS SP2 AOBS, USA) (Fig. 6A and B). One hour after incubation, FAM-conjugated cRGDyK was mainly distributed on the cell surface and in the cytoplasm. Under the same conditions, no fluorescence signal was detected within HSCs in the presence of cRGAyK (data not shown). These results were consistent with no binding of cRGAyK to HSCs. In summary, it is conceivable that HSCs interacted with cRGDyK in a receptor-specific manner and that the interaction was mainly governed by a receptor-mediated endocytotic process.

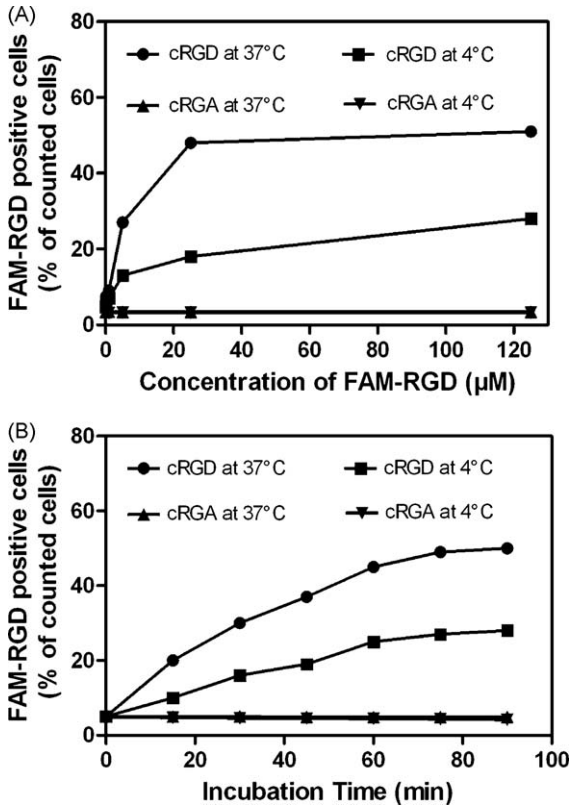

Fig. 5. Binding of FAM-conjugated cRGDyK peptide to HSCs in a dose- and temperature-dependent manner. (A) Binding of activated HSCs with FAM-conjugated cRGDyK peptide in different concentrations at 4 or 37 °C for 60 min. FAM-conjugated cRGAyk peptide was used as a control. FAM-positive cells were counted by flow cytometry after the incubation, and the data are expressed as percentage of counted cells. (B) Binding of activated HSCs with FAM-conjugated cRGDyK peptide at different time points at 4 or 37 °C. $n = 3$ in all groups of each panel.

4. Discussion

Substantial improvements in the diagnosis and treatment of chronic liver disease have accelerated interest in uncovering the mechanisms underlying hepatic fibrosis. Activation of resident hepatic stellate cells into proliferative, contractile, and fibrogenic cells in liver injury remains a dominant theme driving the field.

HSCs are the major producers of the ECM components that accumulate in the liver during the development of hepatic fibrosis [31]. Thus, HSCs are an essential target for the development of diagnostic strategies designed to monitor the activation of HSCs. Selectively targeted binding to HSCs may be beneficial for the diagnosis of liver fibrosis [32].

Integrins are heterodimeric transmembrane glycolproteins, which play an important role in cell-cell and cell-matrix interactions. They belong to a group of cell adhesion molecules consisting of two noncovalently bound transmembrane subunits with large extracellular segments that bind to create heterodimers with distinct adhesive capabilities [9]. Up to now, 18 α and 8 β subunits have been described, which assemble into 24 different receptors. A common feature of many integrins like αvβ3 is that they bind to extracellular matrix proteins via the three amino acid sequence arginine–glycine–aspartic acid (RGD). However, among all 24 integrins discovered to date, the integrin αvβ3 is still the most extensively studied.

Cultured activated human HSCs expressed α1, α2, αv, α6, β1, and β4 integrin subunits [21], while a preliminary study showed that β1 integrin and several α subunits became more highly expressed *in situ* in activated HSCs in human fibrotic liver [33]. Using a well characterized tissue culture model of HSC activation, we showed that rat HSCs express αvβ3 integrin after activation *in vitro*. Detection of αv and β3 integrin in cell lysates by Western blotting showed that the αv subunit was weakly detectable in quiescent rat HSCs. However, both subunits were readily detectable in the activated HSCs. qRT-PCR showed a less dramatic, but significant, increase in αv and β3 integrin mRNA expression following activation of rat HSCs.

Small molecules, e.g., peptides, carbohydrates, or antibody fragments, may ultimately be useful binding ligands. Small peptides have the advantage of being chemically defined, and they are also able to be manufactured in large quantities and at high purity without biological contaminants. They can be selected for specific targets with high affinity and selectivity [34,35]. Small RGD peptides can tolerate harsh conditions for chemical modification. Unlike antibodies, they are less likely to be immunogenic. In the present study, the cyclic pentapeptide RGDyK (Arg-Gly-Asp-DTyr-Lys) was chosen for this purpose. The low molecular mass compound cRGDyK is optimized in size to fit the binding pocket of the αvβ3 integrin receptor [36]. This peptide has been shown to target αvβ3 integrins with high affinity [36].

Here, we have characterized the binding of cRGDyK to purified and membrane-bound integrin αvβ3 receptor expressed on activated hepatic stellate cells (HSCs). We show that both purified and membrane-bound integrin αvβ3 binds to cRGDyK with high affinity. Previous studies have shown that αvβ3 binds to its native

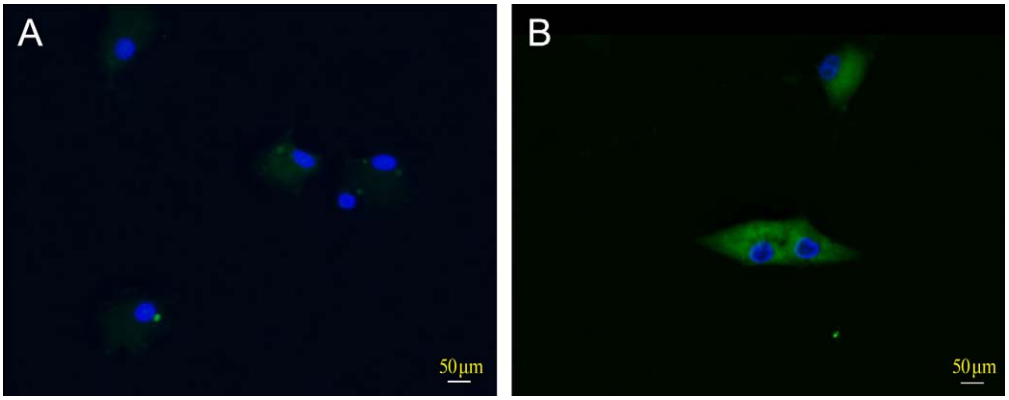

Fig. 6. Affinity of FAM-conjugated cRGDyK peptide with HSCs. (A) Quiescent HSCs with nearly no positive FAM fluorescent signal in the cytoplasm. And they are only positive for DAPI staining in nuclei. (B) FAM-conjugated cRGDyK peptide fluorescent signals were localized within activated HSCs. Activated HSCs are morphologically stellate-like, with many projections. Their cytoplasm was stained in green, and the nucleus was stained in blue by counterstaining with DAPI. (For interpretation of the references to color in this figure legend, the reader is referred to the web version of the article.)

ligand, vitronectin, in a nondissociable manner, whereas an RGD-containing peptide derived from vitronectin binds in a dissociable manner with a K_d of 9.4×10^{-7} M. Our studies indicate that radiolabeled cRGDyK binds to αvβ3 in a dissociable manner, similar to native cyclic RGDyK. These studies demonstrate that cRGDyK binding to αvβ3 is of high affinity and reversible, which is different from vitronectin, and suggests that it may be a useful compound for monitoring activation of HSCs in vitro. The number of αvβ3 receptors expressed on HSCs was about 79,042 sites per cell. In addition, our findings showed that the cRGDyK was coupled to the activated HSCs in a time- and dose-dependent manner.

However, the use of cRGDyK as a targeting peptide for identifying activated HSCs in fibrotic liver may have its limitations. The integrin αvβ3 is an adhesion receptor that is expressed mainly on endothelial cells (ECs), but also on some tumor cells, HSCs, and inflammatory cells, especially monocytes and macrophages [10,37,38]. Until now, there is no report about the expression of αvβ3 on hepatocytes. Flow-cytometric and real-time PCR analysis indicated that expression level of αvβ3 is low in liver sinusoidal endothelial cells (LSEC). [39] There is no detectable αvβ3 on lymphocytes in vitro or in vivo [40]. The expression of αvβ3 is limited to a subset of dendritic cells [41]. Hence, it may be less effective to detect the progression of fibrosis by selectively targeted binding to HSCs with cRGDyK *in vivo*. Validation of this method was hindered by the lack of adequate evidence to confirm the correlation between expression of integrin αvβ3 and the degree of fibrogenesis. Another question is that the binding affinity of cRGDyK for other integrins that may contain either αv or β3 subunit alone must be determined to confirm the selectivity of this peptide as a targeting agent. Previous study showed that only integrin αvβ3 was increased in activated hepatic stellate cells and no studies has shown other integrins was increased in activated HSCs. These issues about the expression of αvβ3 on hepatocytes as compared to other nonparenchymal cells in the liver and the reciprocal selectivity of cRGDyK for αvβ3, as well as for HSC, need further investigations.

In conclusion, the present study demonstrated that: (1) activated HSCs expressed detectable level of integrin αvβ3; (2) the binding of cRGDyK to both purified and membrane-bound integrin αvβ3 was of high affinity and reversible; (3) cRGDyK is taken up by activated HSCs *in vitro* via receptor-mediated endocytosis. Thus, the cRGDyK peptide is a molecule potentially useful for the diagnosis of liver fibrosis.

Conflict of interest

The authors declare no conflict of interest.

Acknowledgements

This project was supported by the National Natural & Science Foundation of China (30770970). We would like to thank Prof. Jian Wu in the Department of Internal Medicine, Division of Gastroenterology & Heaptology, UC Davis Medical Center, Sacramento, CA, USA for critical comments regarding this manuscript.

References

[1] Beljaars L, Meijer DK, Poelstra K. Targeting hepatic stellate cells for cell-specific treatment of liver fibrosis. Front Biosci 2002;7:e214–22.
[2] Wu J, Nantz MH, Zern MA. Targeting hepatocytes for drug and gene delivery: emerging novel approaches and applications. Front Biosci 2002;7:d717–25.
[3] Guma FCR, Mello TG, Mermelstein CS, Fortuna VA, Wofchuk ST, Gottfried C, et al. Intermediate filaments modulation in an in vitro model of the hepatic stellate cell activation or conversion into the lipocyte phenotype. Biochem Cell Biol 2001;79(4):409–17.
[4] de Aguirres AB, Mello PA, Andrade CM, Breier AC, Margis R, Guaragna RM, et al. Variations of ganglioside biosynthetic pathways in the phenotype conversion from myofibroblasts to lipocytes in murine hepatic stellate cell line. Mol Cell Biochem 2007;303(September (1–2)):121–30.
[5] Andrade CM, Roesch GC, Wink MR, Guimarães EL, Souza LF, Jardim FR, et al. Activity and expression of ecto-5′-nucleotidase/CD73 are increased during phenotype conversion of a hepatic stellate cell line. Life Sci 2008;82(January (1–2)):21–9.
[6] Burt AD. Cellular and molecular aspects of hepatic fibrosis. J Pathol 1993; 170:105–14.
[7] Ramm GA, Britton RS, O'Neill R, Blaner WS, Bacon BR. Vitamin A-poor lipocytes: a novel desmin-negative lipocyte subpopulation, which can be activated to myofibroblasts. Am J Physiol 1995;269:G532–41.
[8] Benyon RC, Arthur MJ. Mechanisms of hepatic fibrosis. J Pediatr Gastroenterol Nutr 1998;27:75–85.
[9] Ruoslahti E. RGD and other recognition sequences for integrins. Ann Rev Cell Dev Biol 1996;12:697–715.
[10] Hood JD, Cheresh DA. Role of integrins in cell invasion and migration. Nat Rev Cancer 2002;2:91–100.
[11] Bach-Gansmo T, Danielsson R, Saracco A, Wilczek B, Bogsrud TV, Fangberget A, et al. Integrin receptor imaging of breast cancer: a proof-of-concept study to evaluate 99mTc-NC100692. J Nucl Med 2006;47:1434–9.
[12] Cai W, Wu Y, Chen K, Cao Q, Tice DA, Chen X. In vitro and in vivo characterization of ^{64}Cu-labeled Abegrin, a humanized monoclonal antibody against integrin αvβ3. Cancer Res 2006;66:9673–81.
[13] Haubner R, Wester HJ, Burkhart F, Senekowitsch-Schmidtke R, Weber W, Goodman SL, et al. Glycosylated RGD-containing peptides: tracer for tumor targeting and angiogenesis imaging with improved biokinetics. J Nucl Med 2001;42:326–36.
[14] Haubner R, Kuhnast B, Mang C, Weber WA, Kessler H, Wester HJ, et al. [18F]Galacto-RGD: synthesis, radiolabeling, metabolic stability, and radiation dose estimates. Bioconjug Chem 2004;15:61–9.
[15] Hu G, Lijowski M, Zhang H, Partlow KC. Imaging of Vx-2 rabbit tumors with αvβ3-integrin-targeted ^{111}In nanoparticles. Int J Cancer 2007;120: 1951–7.
[16] Sipkins DA, Cheresh DA, Kazemi MR, Nevin LM, Bednarski MD, Li KC. Detection of tumor angiogenesis in vivo by αvβ3-targeted magnetic resonance imaging. Nat Med 1998;4:623–6.
[17] Winter PM, Caruthers SD, Kassner A, Harris TD. Molecular imaging of angiogenesis in nascent Vx-2 rabbit tumors using a novel αvβ3-targeted nanoparticle and 1.5 Tesla magnetic resonance imaging. Cancer Res 2003;63:5838–43.
[18] Schmieder AH, Winter PM, Caruthers SD, Harris TD. Molecular MR imaging of melanoma angiogenesis with αvβ3-targeted paramagnetic nanoparticles. Magn Reson Med 2005;53:621–7.
[19] Ellegala DB, Leong-Poi H, Carpenter JE, Klibanov AL. Imaging tumor angiogenesis with contrast ultrasound and microbubbles targeted to αvβ3. Circulation 2003;108:336–41.
[20] Chen X, Conti PS, Moats RA. In vivo near-infrared fluorescence imaging of integrin alpha v beta 3 in brain tumor xenografts. Cancer Res 2004;64:8009–14.
[21] Carloni V, Romanelli RG, Pinzani M, Laffi G, Gentilini P. Expression and function of integrin receptors for collagen and laminin in cultured human hepatic stellate cells. Gastroenterology 1996;110:1127–36.
[22] Zhou X, Murphy FR, Gehdu N, Zhang J, Iredale JP, Benyon RC. Engagement of alpha v beta 3 integrin regulates proliferation and apoptosis of hepatic stellate cells. J Biol Chem 2004;279:23996–4006.
[23] Milliano MT, Luxon BA. Initial signaling of the fibronectin receptor (alpha 5 beta 1 integrin) in hepatic stellate cells is independent of tyrosine phosphorylation. J Hepatol 2003;39:32–7.
[24] Zhou X, Zhang Y, Zhang J, Zhu H, Du W, Zhang X, et al. Expression of fibronectin receptor, integrin alpha 5 beta 1 of hepatic stellate cells in rat liver fibrosis. Chin Med J (Engl) 2000;113:272–6.
[25] Levine D, Rockey DC, Milner TA, Breuss JM, Fallon JT, Schnapp LM. Expression of the integrin alpha 8 beta 1 during pulmonary and hepatic fibrosis. Am J Pathol 2000;156:1927–35.
[26] Haubner R, Finsinger D, Kessler H. Stereoisomeric peptide libraries and peptidomimetics for designing selective inhibitors of the αvβ3 integrin for a new cancer therapy. Angew Chem Int Ed Engl 1997;36: 1374–89.
[27] Chen X, Park R, Shahinian AH, Bading JR, Conti PS. Pharmacokinetics and tumor retention of ^{125}I-labeled RGD peptide are improved by PEGylation. Nucl Med Biol 2004;31:11–9.
[28] Benyon RC, Hovell CJ, Da Gaca M, Jones EH, Iredale JP, Arthur MJ. Progelatinase A is produced and activated by rat hepatic stellate cells and promotes their proliferation. Hepatology 1999;30:977–86.
[29] Ke AW, Shi GM, Zhou J, Wu FZ, Ding ZB, Hu MY, et al. Role of overexpression of CD151 and/or c-Met in predicting prognosis of hepatocellular carcinoma. Hepatology 2009;49(February (2)):491–503.
[30] Orlando RA, Cheresh DA. Arginine–glycine–aspartic acid binding leading to molecular stabilization between integrin αvβ3 and its ligand. J Biol Chem 1991;266:19543–50.
[31] Iredale JP. Cirrhosis: new research provides a basis for rational and targeted treatments. BMJ 2002;327:143–7.
[32] Wu J, Zern MA. Hepatic stellate cells: a target for the treatment of liver fibrosis. J Gastroenterol 2000;35(9):665–72.
[33] Reeves HL, Dack CL, Day CP, Burt AD. In: Wisse E, Knook DL, Balabaud C, editors. Cells of the hepatic sinusoid: proceedings of the eighth international

symposium on cells of the hepatic sinusoid, vol. 6. Leiden, The Netherlands: The Kupffer Cell Foundation; 1997. p. 154–5.
[34] Aina OH, Marik J, Liu R, Lau DH, Lam KS. Identification of novel targeting peptides for human ovarian cancer cells using "one-bead one-compound" combinatorial libraries. Mol Cancer Ther 2005;4:806–13.
[35] Du SL, Pan H, Lu WY, Wang J, Wu J, Wang JY. Cyclic Arg-Gly-Asp peptide-labeled liposomes for targeting drug therapy of hepatic fibrosis in rats. J Pharmacol Exp Ther 2007;322:560–8.
[36] Liu S. Radiolabeled cyclic RGD peptides as integrin αvβ3-targeted radiotracers: maximizing binding affinity via bivalency. Bioconjug Chem 2009 [online publication].
[37] Patsenker E, Popov Y, Wiesner M, Goodman SL, Schuppan D. Pharmacological inhibition of the vitronectin receptor abrogates PDGF-BB-induced hepatic stellate cell migration and activation in vitro. J Hepatol 2007;46:878–87.
[38] Chung AS, Gao Q, Kao WJ. Either integrin subunit beta1 or beta3 is involved in mediating monocyte adhesion, IL-1beta protein and mRNA expression in response to surfaces functionalized with fibronectin-derived peptides. J Biomater Sci Polym Ed 2007;18:713–29.
[39] Wu LQ, Zhang WJ, Niu JX, Ye LY, Yang ZH, Grau GE, et al. Phenotypic and functional differences between human liver cancer endothelial cells and liver sinusoidal endothelial cells. J Vasc Res 2008;45(1):78–86.
[40] Edwards S, Lalor PF, Tuncer C, Adams DH. Vitronectin in human hepatic tumours contributes to the recruitment of lymphocytes in an αvβ3-independent manner. Br J Cancer 2006;95(December (11)):1545–54.
[41] Harui A, Roth MD, Vira D, Sanghvi M, Mizuguchi H, Basak SK. Adenoviral-encoded antigens are presented efficiently by a subset of dendritic cells expressing high levels of αvβ3 integrins. J Leukoc Biol 2006;79(June (6)):1271–8.